A&A manuscript no.
(will be inserted by hand later)

Your thesaurus codes are:
(02.12.2;02.13.5; 09.01.1;09.09.1;09.13.2)

ASTRONOMY
AND
ASTROPHYSICS
13.5.1997

Widespread water vapour absorption in SgrB2[1]

J. Cernicharo[1], T. Lim[2], P. Cox[3], E. González-Alfonso[4,5], E. Caux[6], B.M. Swinyard[7], J. Martín-Pintado[5], J.P. Baluteau[8], P. Clegg[9]

[1] CSIC, IEM, Dpto. Física Molecular, Serrano 123, E-28006 Madrid, Spain
[2] The LWS Instrument-Dedicated Team, ISO Science Operations Centre. PO Box 50727, E-28080 Madrid, Spain
[3] Institut d'Astrophysique Spatiale, Bât. 121, Université de Paris XI, F-91405 Orsay Cedex, France
[4] Universidad de Alcalá de Henares, Dpto. Física, Campus Universitario, E-28871 Alcalá de Henares, Spain
[5] Observatorio Astronómico Nacional, Apartado 1143, E-28800 Alcalá de Henares, Spain
[6] Centre d'Etude Spatiale des Rayonnements. CESR/CNRS-UPS, BP 4346, F-31029 Toulouse Cedex. France
[7] Rutherford Appleton Lab., Chilton, Didcot, Oxon OX11 OQX. UK
[8] Laboratoire d'Astronomie Spatiale, LP CNRS, BP 8, F-13376 Marseille Cedex 12, France
[9] Queen Mary and Westfield College, University of London, Mile End Road, London E1 4NS, UK

Received Dec 1996 ; accepted 29^{th} April 1997.

Abstract. We report the discovery of widespread water vapour absorption in the 2_{12}-1_{01} 179.5 μm transition toward the SgrB2 molecular cloud. The data were obtained with the Long Wavelength Spectrometer (LWS) on board the ISO satellite. A raster map centered on SgrB2 made with the LWS grating clearly shows the 179.5 μm H_2O line in absorption against the far-infrared continuum at all observed positions with a line absorption depth of $\sim$ 15%. The grating data are complemented with Fabry-Perot observations of the H_2O 179.5 and 174.6 μm lines, and the $H_2^{18}O$ 181.05 μm. The transitions connecting the ground level show a broad absorption profile between −150 and 100 kms^{-1} proving that water vapour is present in the molecular gas along the line of sight toward SgrB2. The H_2O absorption lines probably arise in the tenuous and extended envelope of SgrB2 where collisional excitation is negligible and the excitation is mainly due to absorption of photons emitted by the dust. We derive a lower limit to the H_2O abundance in SgrB2 of 10^{-5}.

Key words: Line : Identification – Molecular Processes – ISM : individual objects : Sgr B2 – ISM : molecules

1. Introduction

Water vapour, one of the first molecules observed in radio astronomy, was discovered in 1962 by Cheung et al. through the maser emission of its 6_{16}-5_{23} rotational transition at 22 GHz. Since then, many lines of H_2O have been observed at submillimeter wavelengths from the ground. However, all these lines are masering which renders the interpretation of the data difficult (Cernicharo et al. 1990; Menten & Melnick 1991). Recently, Cernicharo et al. (1994, 1996) and González-Alfonso et al. (1995) have mapped the H_2O 183.3 GHz transition in three star-forming regions (Orion-IRC2, HH7-11, and W49N) providing the first evidence that the distribution of water vapour is extended and that the H_2O abundance can be larger than 10^{-5} in warm molecular clouds.

In this Letter, we present further evidence that water vapour is extended in molecular clouds based on the detection of far-infrared H_2O transitions seen in absorption against the continuum of the SgrB2 molecular complex.

2. Observations and results

The observations have been carried out with the LWS spectrometer (Clegg et al. 1996) on board the ISO satellite as part of our open time programs. The LWS grating spectra of SgrB2 were obtained during revolution 287 using the AOT LWS01. The spectra consist of 3 grating scans taken with 0.5 sec integration ramps at each commanded grating position and were oversampled at 1/4 of a resolution element. The flux calibration of the spectra is relative to Uranus (Swinyard et al. 1996). The total on-target time was 2775 sec for each raster (north-south and east-west and centered on SgrB2) of 7 points each with a 90″ spacing. The data have been corrected for the interference pattern which is systematically seen in the LWS

Send offprint requests to: J. Cernicharo

[1] Based on observations with ISO, an ESA project with instruments funded by ESA Member States (especially the PI countries: France Germany, the Netherlands and the United Kingdom) and with the participation of ISAS and NASA.

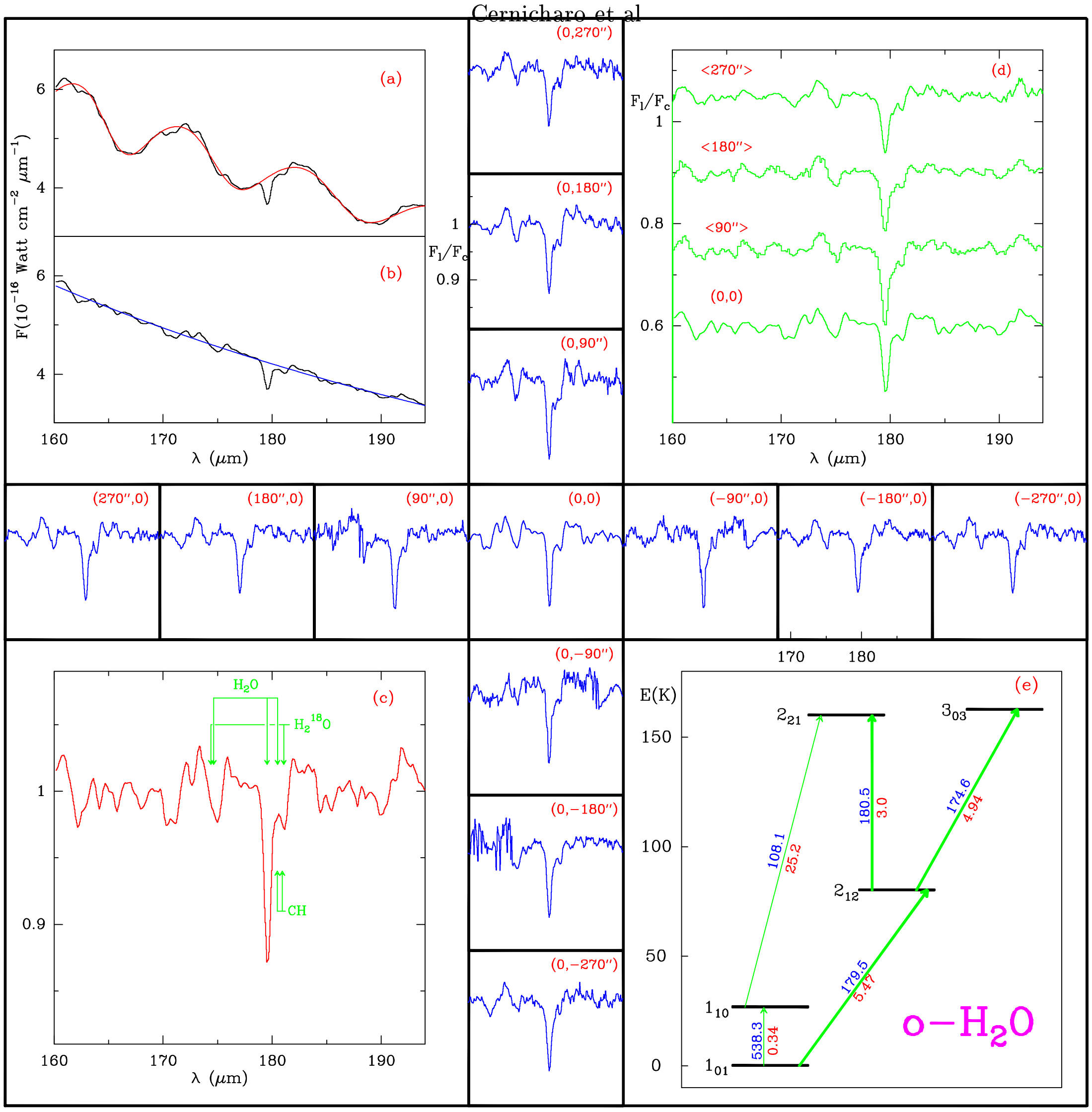

Fig. 1. Raster map obtained with the LWS grating spectra around the $2_{12}-1_{01}$ transition of water vapour at 179.5 μm. The offset positions are given in arcsec in each box of the raster and the central position corresponds to: 17^h 47^m 20.4^s, -28^o 23′ 32.2″ (J 2000). The X axis is the wavelength (168–196 μm) and the Y axis is the line over continuum flux ratio. The spectrum of the central position is shown before the correction of the interference pattern (continuous line) in (a) and after the correction in (b) –the continuous line is the continuum level. The bottom left insert (c) shows the resulting spectrum in the central position divided by the continuum. The top right insert (d) shows the averaged spectrum for offsets 270″, 180″, 90″ and 0″. The bottom right insert (e) presents the ortho water energy levels for energies below 200 K. The allowed radiative transitions are indicated by arrows with the wavelength in microns (left) and the Einstein coefficients in units of 0.01 s (right)

grating spectra of extended sources or point sources which are offset from the optical axis (Swinyard et al. 1996) - see Figs. 1a and b. The central position was also observed at higher spectral resolution in two H_2O, one $H_2{}^{18}O$ and two OH lines using the LWS Fabry-Perot (AOT LWS04) during revolution 322. The spectra were over-sampled at 1/2 of a resolution element yielding a spectral resolution of $\simeq$ 30 kms^{-1}. All data used in this Letter have been processed through the LWS Pipeline Version 6.0.

The grating spectrum toward the central position shows the continuum of the dust emission plus a series of absorption lines (Fig. 1b). The strongest absorption at 179.5 μm corresponds to the water vapour 2_{12}–1_{01} ortho transition. To illustrate the line content of the spectra, Fig. 1c displays the 160 to 196 μm line over continuum ratio of SgrB2. The grating spectra at positions offset from SgrB2 are shown in the central part of Fig. 1. The most striking result from the raster map toward SgrB2 is the presence of the water vapour 179.5 μm line in absorption in all the positions observed. At the resolution of the grating ($\sim$1000 km s^{-1}), the absorption remains strong and roughly constant over the raster with an absorption depth of $\sim$ 15%, consistent with saturated water vapour lines with a line width of $\sim$150 kms^{-1}. The 3_{03}-2_{12} H_2O transition at 174.5 μm is also present in all the raster positions with an absorption depth of 1%. The absorption at

180.5 μm (detected in each position) could be a blend of the 2_{21}–2_{12} H_2O transition at 180.488 μm, the CH line at 180.478 μm and the 2_{12}–1_{01} $H_2^{18}O$ line at 181.05 μm. The other absorption features present in the spectra are seen in all the individual scans and observed positions, although many of them are stronger towards the central position (Fig. 1c). Some of them could be real but further analysis is required to assess their reality. We note that transitions of light molecular species and low energy bending modes of polyatomic molecules are expected at these wavelengths.

The Fabry-Perot spectra obtained toward the central position of SgrB2 are presented in Fig. 2. The upper panel shows the H_2O 2_{12}–1_{01} and 3_{13}–2_{12} transitions and the lower panel the 2_{12}–1_{01} transition of the isotope $H_2^{18}O$. For comparison, the middle panel displays the 119 and 84 μm transitions of OH. The OH spectra will be discussed in detail in a forthcoming paper. The 179.5 μm transition of water vapour, whose lower energy level is the o-H_2O ground state (Fig. 1e), is seen in absorption at all velocities between −150 and 100 km s^{-1}. The line is saturated as expected from the grating spectrum. The $H_2{}^{18}O$ transition is also detected over a wide velocity range (–50 to 80 kms^{-1}). Water vapour is thus detected in absorption not only at the velocities corresponding to the SgrB2 complex but also at more negative velocities which trace the gas along the line of sight toward SgrB2. This is similar to the OH transitions at 119 and 84 μm (Fig. 2d - see also Storey et al. 1981). In contrast, the 174.6 μm H_2O is only detected at 60 km s^{-1}, the velocity of SgrB2.

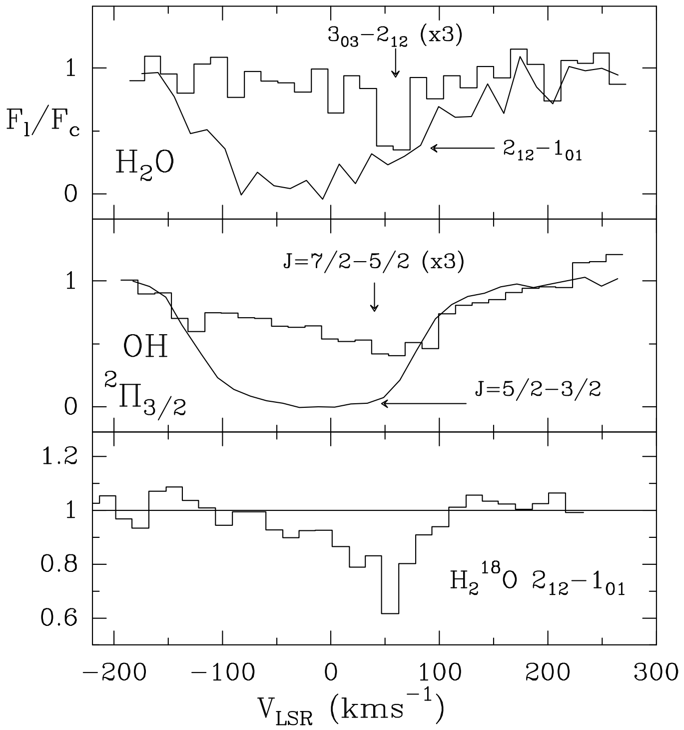

Fig. 2. LWS Fabry-Perot observations of the central position of SgrB2. (a) The 2_{12}-1_{01} and 3_{03}-2_{12} lines of water at 179.52 and 174.6 μm, respectively; (b) the 5/2-3/2 and 7/2-3/2 lines of the $^2\Pi_{3/2}$ state of OH at 119 and 84 μm; (c) the 2_{12}-1_{01} $H_2{}^{18}O$ line at 181.05 μm

3. Discussion

The main result from the present observations is that the far-infrared lines of water vapour are seen in absorption toward SgrB2, instead of in emission. Similar results are reported for other galactic molecular clouds by Cox et al. (1997). This suggests that in SgrB2, where the continuum emission in the far-infrared is optically thick (see below), the H_2O lines arise in a region where the excitation temperatures are smaller than the dust temperature ($\sim$ 30 K). Nevertheless, the problem of H_2O line excitation is not simple because, apart from self-absorption and the possibility of collisional excitation, the excitation temperatures will also be affected by the continuum emission of the dust. The role of dust is essential in the excitation of molecules such as H_2O which have transitions at far- and near-infrared wavelengths, and must be taken into account in any realistic model of line excitation.

In the following, we present a simple model to define the conditions for which the far-infrared H_2O lines appear in absorption and to quantify the depth of the absorption lines. The model assumes a uniform and spherical cloud, with the following physical parameters appropriate for SgrB2 (see Baluteau et al. 1997 and references therein): an H_2 column density of $N(H_2)= 10^{24}$ cm^{-2}, a dust to gas abundance of 10^{-2} by mass, a grain radius 0.1 μm, an absorption efficiency $Q_\lambda = 2\pi a_g/\lambda$, a dust temperature T_d=30 K, a turbulent velocity V_{tur} = 10 km s^{-1}. The H_2 density $n(H_2)$, the kinetic temperature T_k, and the water abundance are free parameters. The dust continuum observed in the LWS wavelength range is well reproduced with the above parameters (Fig. 3c). The continuum opacities are 3.5 and 1.9 at 100 and 180 μm respectively. The models compute the statistical equilibrium populations of the seven lowest levels of o-H_2O. The collisional coefficients are taken from Green et al. (1993) and the excitation by dust emission is treated by assuming that the dust grains and the water molecules are coexistent (González-Alfonso & Cernicharo, in preparation).

Figs. 3a and b display for the four lowest o-H_2O transitions with wavelengths in the LWS range the line over continuum flux ratio as a function of T_k for two values of $n(H_2)$: 10^5 and 10^6 cm^{-3} and for an abundance of o-H_2O of 10^{-5}. All four lines are very thick across the cloud, with maximum opacities always greater than 10^3. The lowest lying 2_{12}-1_{01} line at 179.5 μm has an opacity greater than 5 10^4 and its line over continuum flux ratio varies significantly with T_k. Fig. 3 indicates that the H_2O lines are seen in absorption only if T_k is below 35 and 30 K for $n(H_2)$ = 10^5 and 10^6 cm^{-3}, respectively. Hence, the water vapour lines detected in absorption originate in the low

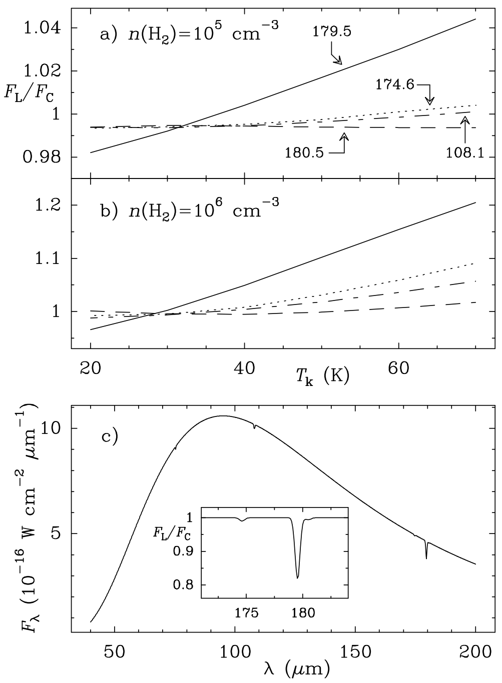

Fig. 3. a) and b) Results of model calculations showing the line over continuum flux ratio of four o-H_2O transitions (labelled with their wavelengths) as a function of kinetic temperature. c) Model spectrum for a cloud with an external absorbing shell (see text for details)

density regions of SgrB2, i.e. the extended and tenuous envelope of the molecular cloud, and not in the inner regions with $T_k \sim 100$ K observed, e.g., in NH_3 (Hüttemeister et al. 1993), where the water lines would be expected to be in emission. With the grating resolution, and even when collisions are neglected, the absorption depths in our models for the 108.1, 174.6 and 180.5 μm lines are always lower than 1 %. This is due to the fact that the dust emission increases the line excitation temperatures to values close to T_d. This result is consistent with the Fabry-Perot observation of the 3_{03}-2_{12} line at 174.6 μm (Fig. 2), which shows an absorption of $\sim$ 20 %. However, the absorption depth of the 2_{12}-1_{01} transition ($\sim$ 15 % in the grating spectra) cannot be explained by this simple model. The reason is that the observed velocity coverage of this line is $\sim$ 200 km s^{-1} (Fig. 2), indicating that low excitation molecular clouds along the line of sight toward SgrB2 also contribute to the absorption. The excitation of the H_2O molecules in these intervening clouds must be low since the 3_{03}-2_{12} absorption line is not detected at velocities below 20 km s^{-1} (Fig. 2b). This is further confirmed by the lack of reemission of the 2_{12}-1_{01} line at those velocities. We have added to the previous model (with $n(H_2)=10^5$ cm^{-3} and $T_k = 20$ K) an absorbing shell located between the observer and the SgrB2 model cloud. The parameters of this shell are the same as for the SgrB2 cloud except that $N(H_2)=10^{21}$ cm^{-2} and $V_{tur} = 40$ km s^{-1}. Since the absorbing shell is optically thin in the continuum, the excitation temperatures are low and there is only appreciable absorption in the 179.5 μm line. Fig. 3c presents the resulting grating spectrum and the insert panel shows the line over continuum ratio around 180 μm.

The present observations confirm the previous suggestion made by Cernicharo et al. (1994) that water vapour exits in large amounts in the direction of molecular clouds. However, the large opacity of the infrared H_2O lines detected in SgrB2 makes any estimate of the water abundance difficult. Our models indicate that the $H_2^{18}O$ 2_{12}-1_{01} line must also be thick in order to explain the line absorption at 181.05 μm. Nevertheless, we note that the depth of the absorption is still sensitive to the optical depth even if the line is thick, because the velocity range where the line can absorb the continuum emission increases with the opacity. Hence, our simple models can derive the $H_2^{18}O$ abundance from the observed absorption depth at 181.05 μm. The value depends on the assumed velocity dispersion in the cloud. Adopting $V_{tur} \leq 20$ km s^{-1}, $N(H_2)=10^{23}$ cm^{-2}, $[H_2O]/[H_2^{18}O]$=500 and neglecting collisional excitation, i.e. all the rotational levels are excited by infrared photons from the dust, we derive a lower limit for the water abundance in SgrB2 of 10^{-5}.

Finally, the $H_2^{18}O$ line profile in Fig. 2 shows an absorption of 10% between -50 and 50 kms^{-1}. This absorption is produced in the low density gas associated with the molecular ring around the galactic center. Assuming that all the absorbing molecules are in the ground state, we derive N($H_2^{18}O$)$\sim$5 10^{13} cm^{-2} and N(H_2O)$\sim$3 10^{16}cm^{-2}. Assuming gas column densities of 10^{21}-10^{22} cm^{-2} the water vapour abundance in the clouds along the line of sight of SgrB2 is $\sim$0.1-1 10^{-5}.

References

Baluteau, J.P. et al. 1997, AA, in press

Cernicharo J., Thum C., Hein H., Garcia P., & Mattiocco F. 1990, AA 231, L15.

Cernicharo J., González-Alfonso E., Alcolea J., Bachiller R., & John D. 1994, ApJ, 432, L59.

Cernicharo J., Bachiller R., & González-Alfonso E. 1996, AA, 305, L5.

Cheung A.C., Rank D.M., Townes C.H., Thornton D.D., & Welch W.J. 1969, Nature, 221, 626

Clegg et al., 1996, AA, 315, L38

Cox, P. et al. 1997, AA, this volume

González-Alfonso E., Cernicharo J., Bachiller R., & Fuente A. 1995, AA, 293, L9

Green, S., Maluendes, S., & McLean, A.D. 1993, ApJS, 85, 181

Hüttemeister S., Wilson T.L., Henkel et al, 1993, AA, 276, 445

Menten, K., & Melnick, G.J. 1991, ApJ, 377, 647

Storey, J., Watson, D.M., Townes, C.H.:1981, ApJ, 244, L27

Swinyard et al., 1996, AA, 315, L43

This article was processed by the author using Springer-Verlag LaTeX A&A style file *L-AA* version 3.